

FEATURES

Single-supply operation

- Output swings rail-to-rail
- Input voltage range extends below ground
- Single-supply capability from 3 V to 36 V

High load drive

- Capacitive load drive of 470 pF ($G = +1$, 25% overshoot)
- Linear output current of 40 mA, 0.5 V from supplies

Excellent ac performance on 2.6 mA/amplifier

- 3 dB bandwidth of 17 MHz, $G = +1$
- 325 ns settling time to 0.01% (2 V step)
- Slew rate of 30 V/ μ s
- Low distortion: -108 dBc at 20 kHz ($G = -1$, $R_L = 2$ k Ω)

Good dc performance

- 700 μ V maximum input offset voltage
- 1 μ V/ $^{\circ}$ C offset voltage drift
- 25 pA maximum input bias current

Low noise: 14 nV/ $\sqrt{\text{Hz}}$ at 10 kHz

No phase inversion with inputs to the supply rails

APPLICATIONS

- Photodiode preamps
- Active filters
- 12-bit to 16-bit data acquisition systems
- Medical instrumentation
- Precision instrumentation

GENERAL DESCRIPTION

The **AD823A** is a dual precision, 17 MHz, JFET input op amp manufactured in the extra fast complementary bipolar (XFCB) process. The **AD823A** can operate from a single supply of 3 V to 36 V or from dual supplies of ± 1.5 V to ± 18 V. It has true single-supply capability with an input voltage range extending below ground in single-supply mode. Output voltage swing extends to within 20 mV of each rail for $I_{OUT} \leq 100$ μ A, providing outstanding output dynamic range. It also has a linear output current of 40 mA, 0.5 V from the supply rails.

An offset voltage of 700 μ V maximum, an offset voltage drift of 1 μ V/ $^{\circ}$ C, and typical input bias currents of 0.3 pA provide dc precision with source impedances up to 1 G Ω . The **AD823A** provides 17 MHz, -3 dB bandwidth, and a 30 V/ μ s slew rate with a low supply current of only 2.6 mA per amplifier. It also provides low input voltage noise of 14 nV/ $\sqrt{\text{Hz}}$ and -108 dB SFDR at 20 kHz. The **AD823A** has low input capacitances (0.6 pF differential and 1.3 pF common mode) and drives more than 500 pF of direct capacitive load as a follower. This lets the amplifier handle a wide range of load conditions.

Rev. B

Information furnished by Analog Devices is believed to be accurate and reliable. However, no responsibility is assumed by Analog Devices for its use, nor for any infringements of patents or other rights of third parties that may result from its use. Specifications subject to change without notice. No license is granted by implication or otherwise under any patent or patent rights of Analog Devices. Trademarks and registered trademarks are the property of their respective owners.

CONNECTION DIAGRAM

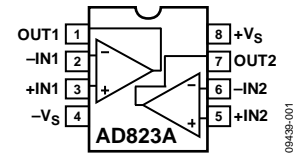


Figure 1. 8-Lead SOIC

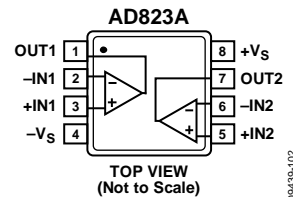


Figure 2. 8-Lead MSOP

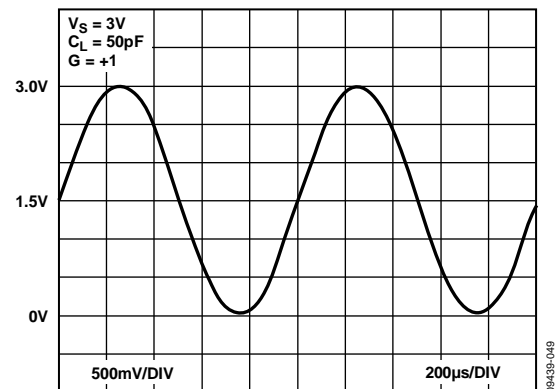


Figure 3. Output Swing, $+V_S = +3$ V, $G = +1$

This combination of ac and dc performance, plus the outstanding load drive capability, results in an exceptionally versatile amplifier for applications such as ADC drivers, high speed active filters, and other low voltage, high dynamic range systems.

The **AD823A** is available over the industrial temperature range of -40° C to $+85^{\circ}$ C and is offered in an 8-lead SOIC package and an 8-lead MSOP package.

AD823A* Product Page Quick Links

Last Content Update: 11/01/2016

Comparable Parts

View a parametric search of comparable parts

Evaluation Kits

- Universal Evaluation Board for Dual High Speed Operational Amplifiers

Documentation

Data Sheet

- AD823A: Wide Supply Dual, 17 MHz, Rail-to-Rail FET Input Amplifier Datasheet

User Guides

- UG-128: Universal Evaluation Board for Dual High Speed Op Amps in SOIC Packages
- UG-886: Universal Evaluation Board for Dual High Speed Op Amps Offered in 8-Lead MSOP

Tools and Simulations

- Analog Filter Wizard
- Analog Photodiode Wizard
- AD823A SPICE Macro-Model

Design Resources

- AD823A Material Declaration
- PCN-PDN Information
- Quality And Reliability
- Symbols and Footprints

Discussions

View all AD823A EngineerZone Discussions

Sample and Buy

Visit the product page to see pricing options

Technical Support

Submit a technical question or find your regional support number

TABLE OF CONTENTS

Features	1	Pin Configuration and Function Descriptions.....	7
Applications.....	1	Typical Performance Characteristics	8
General Description	1	Theory of Operation	14
Connection Diagram	1	Output Impedance	14
Revision History	2	Applications Information	15
Specifications.....	3	Input Characteristics.....	15
5 V Operation	3	Output Characteristics.....	15
3.3 V Operation	4	Wideband Photodiode Preamp	16
± 15 V Operation.....	5	Active Filter	18
Absolute Maximum Ratings.....	6	Maximizing Performance Through Proper Layout.....	19
Thermal Resistance	6	Outline Dimensions	20
ESD Caution.....	6	Ordering Guide	20

REVISION HISTORY

6/12—Rev. A to Rev. B

Added Text to Absolute Maximum Ratings Section.....	6
Changes to Equation 8	18

5/12—Revision A: Initial Version

SPECIFICATIONS

5 V OPERATION

$T_A = 25^\circ\text{C}$, $+V_S = 5\text{ V}$, $R_L = 2\text{ k}\Omega$ to 2.5 V , unless otherwise noted.

Table 1.

Parameter	Conditions	Min	Typ	Max	Unit
DYNAMIC PERFORMANCE					
-3 dB Bandwidth	$G = +1$, $V_{OUT} \leq 0.2\text{ V p-p}$	14.1	17		MHz
Full Power Response	$V_{OUT} = 2\text{ V p-p}$		4.8		MHz
Slew Rate	$G = -1$, $V_{OUT} = 4\text{ V step}$	25	30		V/ μs
Settling Time					
To 0.1%	$G = -1$, $V_{OUT} = 2\text{ V step}$		240		ns
To 0.01%	$G = -1$, $V_{OUT} = 2\text{ V step}$		325		ns
NOISE/DISTORTION PERFORMANCE					
Input Voltage Noise	$f = 10\text{ kHz}$		14		nV/ $\sqrt{\text{Hz}}$
Input Current Noise	$f = 1\text{ kHz}$		1		fA/ $\sqrt{\text{Hz}}$
Harmonic Distortion (SFDR)	$V_{OUT} = 2\text{ V p-p}$, $f = 20\text{ kHz}$, $G = -1$, $R_F = R_G = 4\text{ k}\Omega$		-108		dBc
	$V_{OUT} = 2\text{ V p-p}$, $f = 20\text{ kHz}$, $G = +1$, $R_L = 1\text{ k}\Omega$		-99		dBc
Crosstalk					
$f = 1\text{ kHz}$	$R_L = 5\text{ k}\Omega$		-123		dB
$f = 1\text{ MHz}$	$R_L = 5\text{ k}\Omega$		-77		dB
DC PERFORMANCE					
Initial Offset			0.12	0.7	mV
Maximum Offset over Temperature			0.2	1.3	mV
Offset Drift			1		$\mu\text{V}/^\circ\text{C}$
Input Bias Current	$V_{CM} = 0\text{ V to }4\text{ V}$		0.3	25	pA
At T_{MAX}	$V_{CM} = 0\text{ V to }4\text{ V}$		10	25	pA
Input Offset Current			0.3	20	pA
At T_{MAX}			3.5		pA
Open-Loop Gain	$V_{OUT} = 0.2\text{ V to }4\text{ V}$, $R_L = 2\text{ k}\Omega$	40	175		V/mV
T_{MIN} to T_{MAX}		25			V/mV
INPUT CHARACTERISTICS					
Input Common-Mode Voltage Range		-0.2 to +3	-0.2 to +3.8		V
Input Resistance			10^{13}		Ω
Input Capacitance	Differential Mode		0.6		pF
	Common Mode		1.3		pF
Common-Mode Rejection Ratio	$V_{CM} = 0\text{ V to }3\text{ V}$	60	73		dB
OUTPUT CHARACTERISTICS					
Output Voltage Swing					
$I_L = \pm 100\ \mu\text{A}$			0.009 to 4.98		V
$I_L = \pm 2\text{ mA}$			0.026 to 4.96		V
$I_L = \pm 10\text{ mA}$			0.097 to 4.88		V
Linear Output Current	$V_{OUT} = 0.5\text{ V to }4.5\text{ V}$		40		mA
Short-Circuit Current	Sourcing to 2.5 V		50		mA
	Sinking to 2.5 V		101		mA
Capacitive Load Drive	$G = +1$		500		pF
POWER SUPPLY					
Operating Range		3		36	V
Quiescent Current	T_{MIN} to T_{MAX} , total		5.1	5.7	mA
Power Supply Rejection Ratio	$V_S = 5\text{ V to }15\text{ V}$, T_{MIN} to T_{MAX}	70	94		dB

3.3 V OPERATION

$T_A = 25^\circ\text{C}$, $+V_S = 3.3\text{ V}$, $R_L = 2\text{ k}\Omega$ to 1.65 V , unless otherwise noted.

Table 2.

Parameter	Conditions	Min	Typ	Max	Unit
DYNAMIC PERFORMANCE					
-3 dB Bandwidth	$G = +1, V_{OUT} \leq 0.2\text{ V p-p}, V_{CM} = 0.65\text{ V}$	13.8	17.3		MHz
Full Power Response	$V_{OUT} = 2\text{ V p-p}$		3.7		MHz
Slew Rate	$G = -1, V_{OUT} = 2\text{ V step}, V_{CM} = 0.65\text{ V}$	18	23		V/ μs
Settling Time					
To 0.1%	$G = -1, V_{OUT} = 2\text{ V step}$		350		ns
To 0.01%	$G = -1, V_{OUT} = 2\text{ V step}$		460		ns
NOISE/DISTORTION PERFORMANCE					
Input Voltage Noise	$f = 10\text{ kHz}$		14		nV/ $\sqrt{\text{Hz}}$
Input Current Noise	$f = 1\text{ kHz}$		1		fA/ $\sqrt{\text{Hz}}$
Harmonic Distortion (SFDR)	$V_{OUT} = 2\text{ V p-p}, f = 20\text{ kHz}, G = -1, R_F = R_G = 4\text{ k}\Omega$		-108		dBc
	$V_{OUT} = 2\text{ V p-p}, f = 20\text{ kHz}, G = +1, R_L = 100\ \Omega$		-70		dBc
Crosstalk					
$f = 1\text{ kHz}$	$R_L = 5\text{ k}\Omega$		-123		dB
$f = 1\text{ MHz}$	$R_L = 5\text{ k}\Omega$		-77		dB
DC PERFORMANCE					
Initial Offset			0.14	1	mV
Maximum Offset over Temperature			0.3	1.8	mV
Offset Drift			1		$\mu\text{V}/^\circ\text{C}$
Input Bias Current	$V_{CM} = 0\text{ V to }2\text{ V}$		0.3	25	pA
At T_{MAX}	$V_{CM} = 0\text{ V to }2\text{ V}$		10	25	pA
Input Offset Current			0.3	20	pA
At T_{MAX}			3.5		pA
Open-Loop Gain	$V_{OUT} = 0.2\text{ V to }2\text{ V}, R_L = 2\text{ k}\Omega$	16	63		V/mV
T_{MIN} to T_{MAX}		14			V/mV
INPUT CHARACTERISTICS					
Input Common-Mode Voltage Range		-0.2 to +1	-0.2 to +1.8		V
Input Resistance			10^{13}		Ω
Input Capacitance	Differential Mode		0.6		pF
	Common Mode		1.3		pF
Common-Mode Rejection Ratio	$V_{CM} = 0\text{ V to }1\text{ V}$	54	71		dB
OUTPUT CHARACTERISTICS					
Output Voltage Swing					
$I_L = \pm 100\ \mu\text{A}$			0.006 to 3.28		V
$I_L = \pm 2\text{ mA}$			0.04 to 3.26		V
$I_L = \pm 10\text{ mA}$			0.093 to 3.18		V
Linear Output Current	$V_{OUT} = 0.5\text{ V to }2.5\text{ V}$		40		mA
Short-Circuit Current	Sourcing to 1.5 V		44		mA
	Sinking to 1.5 V		86		mA
Capacitive Load Drive	$G = +1$		500		pF
POWER SUPPLY					
Operating Range		3		36	V
Quiescent Current	T_{MIN} to T_{MAX} , total		5.0	5.7	mA
Power Supply Rejection Ratio	$V_S = 3.3\text{ V to }15\text{ V}, T_{MIN}$ to T_{MAX}	70	80		dB

±15 V OPERATION

$T_A = 25^\circ\text{C}$, $V_S = \pm 15\text{ V}$, $R_L = 2\text{ k}\Omega$ to 0 V , unless otherwise noted.

Table 3.

Parameter	Conditions	Min	Typ	Max	Unit
DYNAMIC PERFORMANCE					
-3 dB Bandwidth	$G = +1$, $V_{OUT} \leq 0.2\text{ V p-p}$	16.5	19		MHz
Full Power Response	$V_{OUT} = 2\text{ V p-p}$		5.6		MHz
Slew Rate	$G = -1$, $V_{OUT} = 10\text{ V step}$	31	35		V/ μs
Settling Time					
To 0.1%	$G = -1$, $V_{OUT} = 10\text{ V step}$		380		ns
To 0.01%	$G = -1$, $V_{OUT} = 10\text{ V step}$		510		ns
NOISE/DISTORTION PERFORMANCE					
Input Voltage Noise	$f = 10\text{ kHz}$		13		nV/ $\sqrt{\text{Hz}}$
Input Current Noise	$f = 1\text{ kHz}$		1		fA/ $\sqrt{\text{Hz}}$
Harmonic Distortion (SFDR)	$V_{OUT} = 10\text{ V p-p}$, $f = 20\text{ kHz}$, $G = -1$, $R_F = R_G = 4\text{ k}\Omega$		-101		dBc
	$V_{OUT} = 10\text{ V p-p}$, $f = 20\text{ kHz}$, $G = +1$, $R_L = 600\ \Omega$		-89		dBc
Crosstalk					
$f = 1\text{ kHz}$	$R_L = 5\text{ k}\Omega$		-123		dB
$f = 1\text{ MHz}$	$R_L = 5\text{ k}\Omega$		-77		dB
DC PERFORMANCE					
Initial Offset			0.8	3.5	mV
Maximum Offset over Temperature			1.0	5	mV
Offset Drift			1		$\mu\text{V}/^\circ\text{C}$
Input Bias Current	$V_{CM} = 0\text{ V}$		1.3	25	pA
	$V_{CM} = -10\text{ V}$		3.5		pA
At T_{MAX}	$V_{CM} = 0\text{ V}$		55	95	pA
Input Offset Current			1.3	20	pA
At T_{MAX}			9.5		pA
Open-Loop Gain	$V_{OUT} = +10\text{ V to } -10\text{ V}$, $R_L = 2\text{ k}\Omega$	100	450		V/mV
T_{MIN} to T_{MAX}		80			V/mV
INPUT CHARACTERISTICS					
Input Common-Mode Voltage Range		-15.2 to +13	-15.2 to +13.8		V
Input Resistance			10^{13}		Ω
Input Capacitance	Differential Mode		0.6		pF
	Common Mode		1.3		pF
Common-Mode Rejection Ratio	$V_{CM} = -15\text{ V to } +13\text{ V}$	70	90		dB
OUTPUT CHARACTERISTICS					
Output Voltage Swing					
$I_L = \pm 100\ \mu\text{A}$			-14.9 to +14.96		V
$I_L = \pm 2\text{ mA}$			-14.97 to +14.96		V
$I_L = \pm 10\text{ mA}$			-14.91 to +14.89		V
Linear Output Current	$V_{OUT} = -14.5\text{ V to } +14.5\text{ V}$		44		mA
Short-Circuit Current	Sourcing to 0 V		78		mA
	Sinking to 0 V		124		mA
Capacitive Load Drive	$G = +1$		500		pF
POWER SUPPLY					
Operating Range		3		36	V
Quiescent Current	T_{MIN} to T_{MAX} , total		6.3	8.4	mA
Power Supply Rejection Ratio	$V_S = 5\text{ V to } 15\text{ V}$, T_{MIN} to T_{MAX}	70	94		dB

ABSOLUTE MAXIMUM RATINGS

Table 4.

Parameter	Rating
Supply Voltage	36 V
Power Dissipation	See Figure 4
Input Voltage (Common Mode)	$\pm V_S \pm 0.7$ V
Differential Input Voltage	$\pm V_S$
Output Short-Circuit Duration	See Figure 4
Storage Temperature Range	-65°C to +125°C
Operating Temperature Range	-40°C to +85°C
Lead Temperature (Soldering, 10 sec)	300°C
ESD Ratings (Human Body Model)	4500 V
ESD Ratings (Charged Device Model)	1250 V

Stresses above those listed under Absolute Maximum Ratings may cause permanent damage to the device. This is a stress rating only; functional operation of the device at these or any other conditions above those indicated in the operational section of this specification is not implied. Exposure to absolute maximum rating conditions for extended periods may affect device reliability.

Use the part with caution at the 30 V supply as excessive output current may overheat and damage the part.

THERMAL RESISTANCE

θ_{JA} is specified for the worst-case conditions, that is, a device soldered in a circuit board for surface-mount packages.

The specification is for the device in free air.

Table 5. Thermal Resistance

Package Type	θ_{JA}	Unit
8-Lead SOIC_N	120	°C/W
8-Lead MSOP	133	°C/W

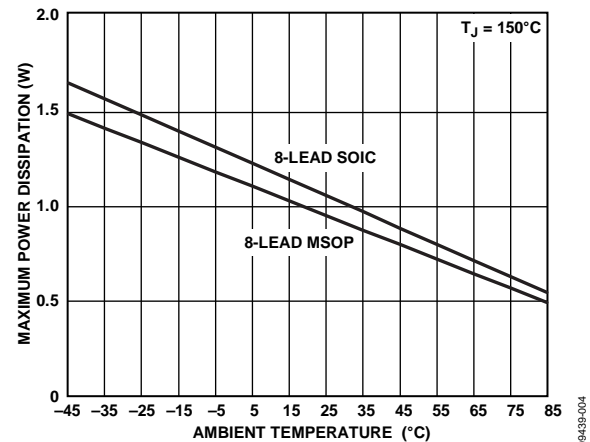


Figure 4. Maximum Power Dissipation vs. Temperature

ESD CAUTION



ESD (electrostatic discharge) sensitive device. Charged devices and circuit boards can discharge without detection. Although this product features patented or proprietary protection circuitry, damage may occur on devices subjected to high energy ESD. Therefore, proper ESD precautions should be taken to avoid performance degradation or loss of functionality.

PIN CONFIGURATION AND FUNCTION DESCRIPTIONS

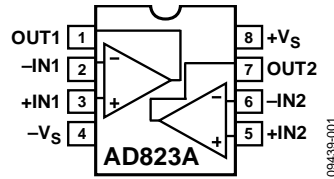


Figure 5. 8-Lead SOIC Pin Configuration

Table 6. Pin Function Descriptions

Pin No.	Mnemonic	Description
1	OUT1	Output 1.
2	-IN1	Inverting Input 1.
3	+IN1	Noninverting Input 1.
4	-Vs	Negative Supply.
5	+IN2	Noninverting Input 2.
6	-IN2	Inverting Input 2.
7	OUT2	Output 2.
8	+Vs	Positive Supply.

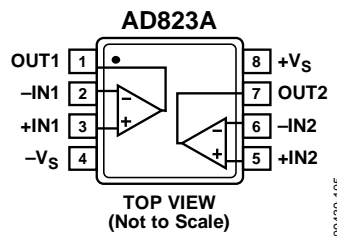


Figure 6. 8-Lead MSOP Pin Configuration

Table 7. Pin Function Descriptions

Pin No.	Mnemonic	Description
1	OUT1	Output 1.
2	-IN1	Inverting Input 1.
3	+IN1	Noninverting Input 1.
4	-Vs	Negative Supply.
5	+IN2	Noninverting Input 2.
6	-IN2	Inverting Input 2.
7	OUT2	Output 2.
8	+Vs	Positive Supply.

TYPICAL PERFORMANCE CHARACTERISTICS

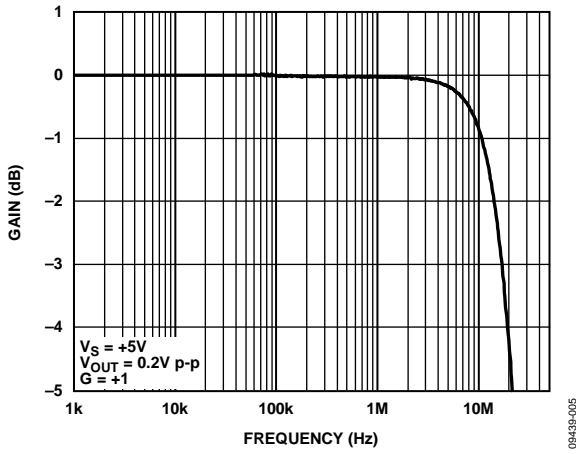


Figure 7. Small Signal Bandwidth, $G = +1$

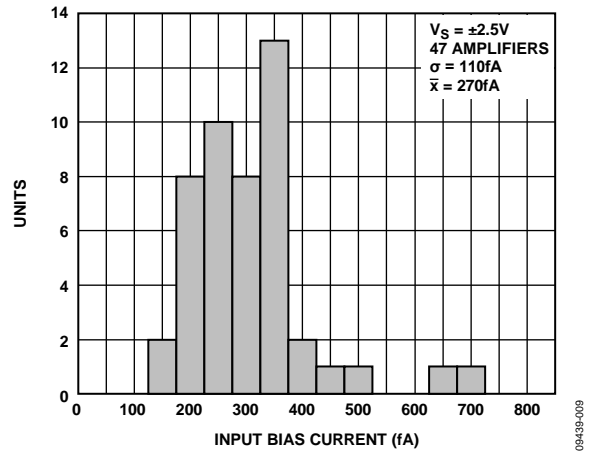


Figure 10. Typical Distribution of Input Bias Current

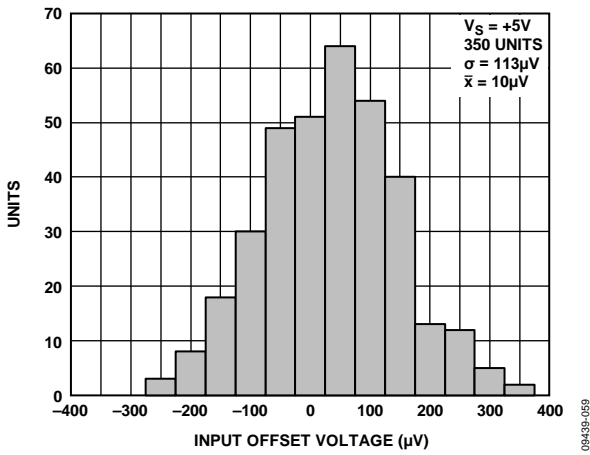


Figure 8. Typical Distribution of Input Offset Voltage

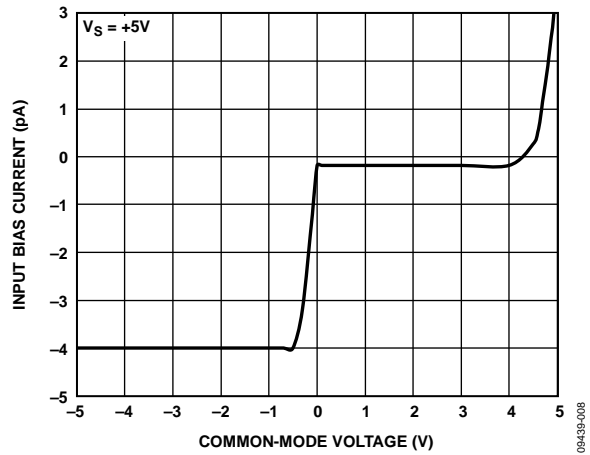


Figure 11. Input Bias Current vs. Common-Mode Voltage

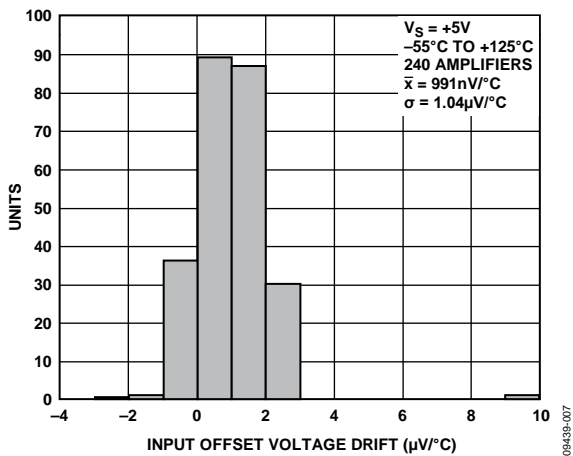


Figure 9. Typical Distribution of Input Offset Voltage Drift

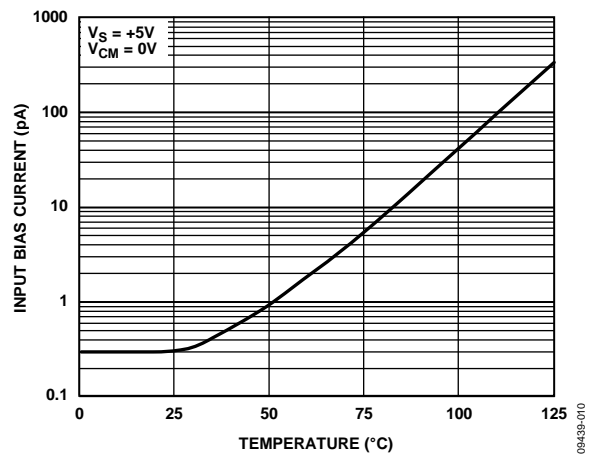


Figure 12. Input Bias Current vs. Temperature

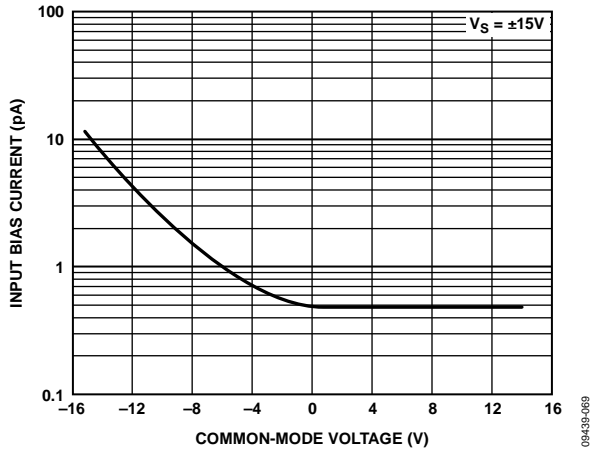


Figure 13. Input Bias Current vs. Common-Mode Voltage

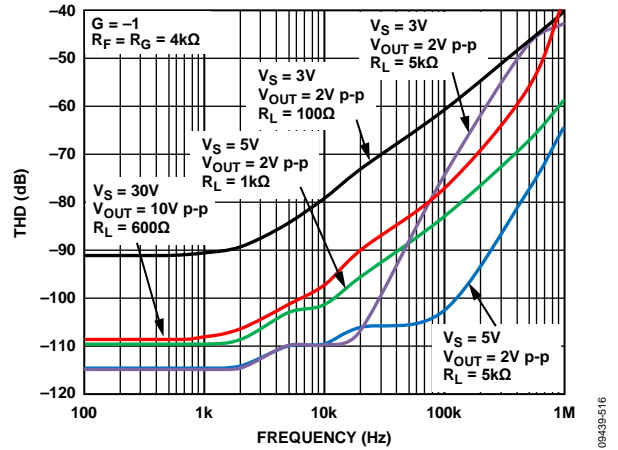


Figure 16. Total Harmonic Distortion vs. Frequency

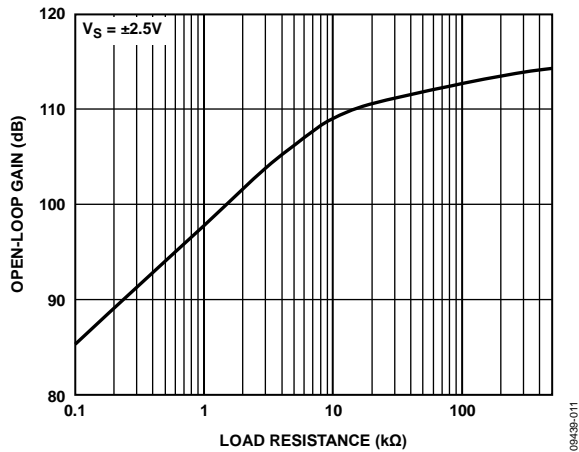


Figure 14. Open-Loop Gain vs. Load Resistance

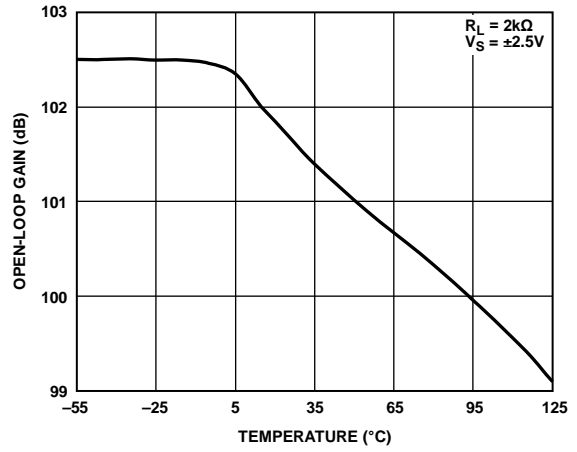


Figure 17. Open-Loop Gain vs. Temperature

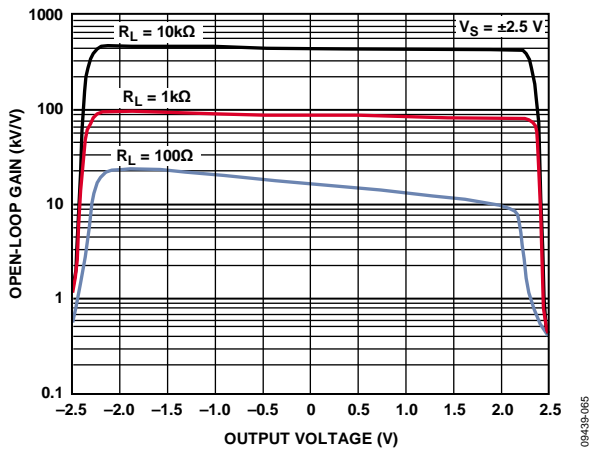


Figure 15. Open-Loop Gain vs. Output Voltage, $V_S = \pm 2.5 V$

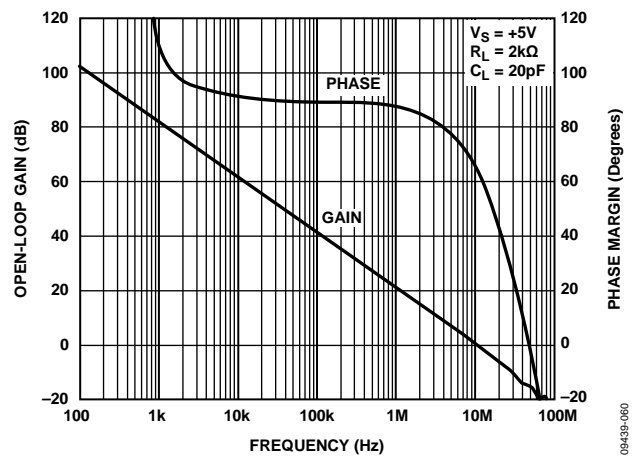


Figure 18. Open-Loop Gain and Phase Margin vs. Frequency

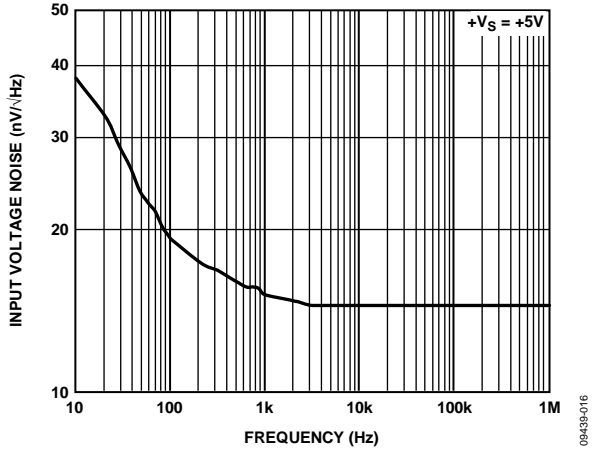


Figure 19. Input Voltage Noise vs. Frequency

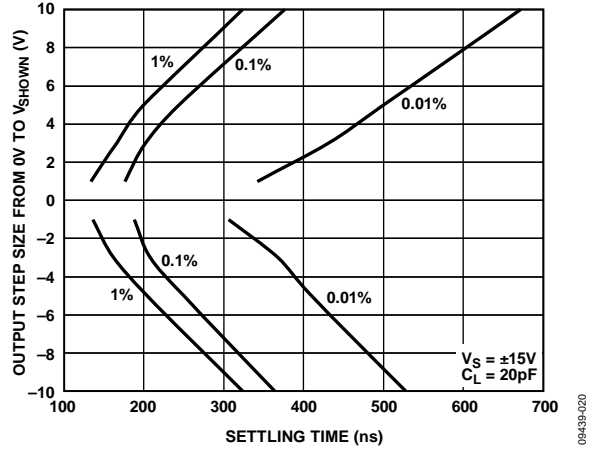


Figure 22. Output Step Size vs. Settling Time (Inverter)

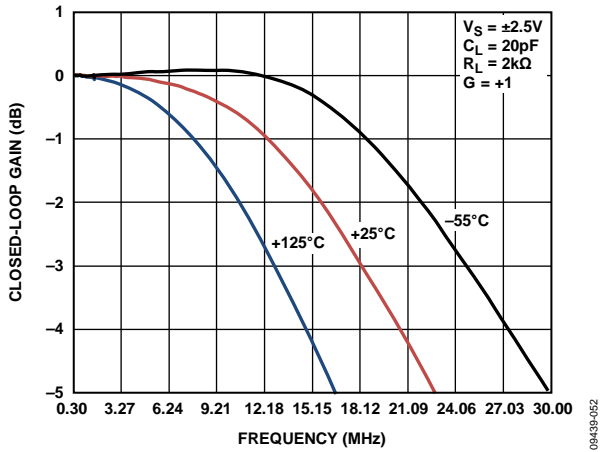


Figure 20. Closed-Loop Bandwidth vs. Temperature

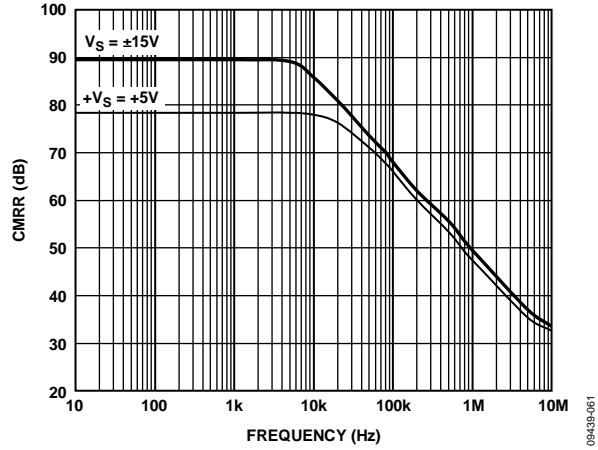


Figure 23. Common-Mode Rejection Ratio vs. Frequency

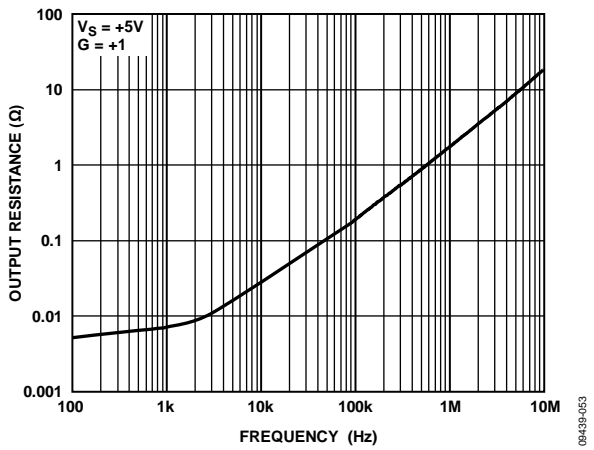


Figure 21. Output Resistance vs. Frequency, +Vs = +5V, G = +1

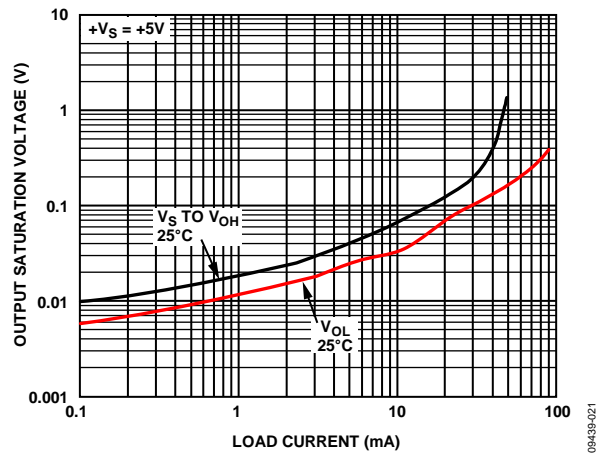


Figure 24. Output Saturation Voltage vs. Load Current

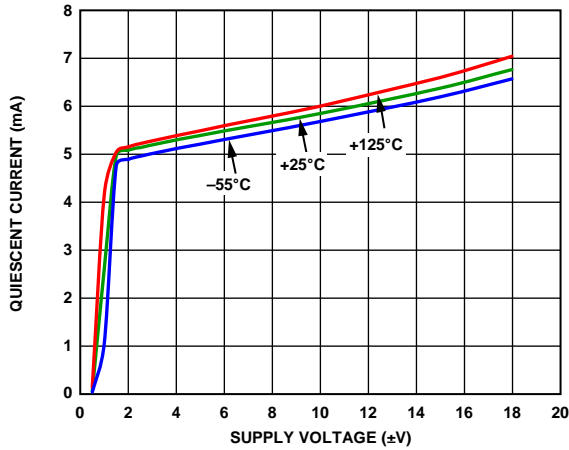


Figure 25. Quiescent Current vs. Supply Voltage

09439-525

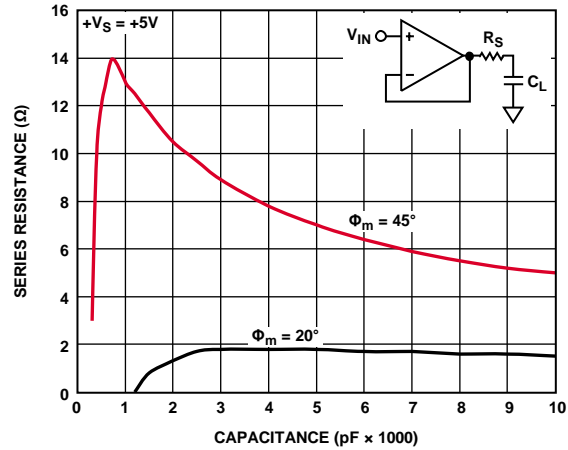


Figure 28. Series Resistance vs. Capacitive Load

09439-067

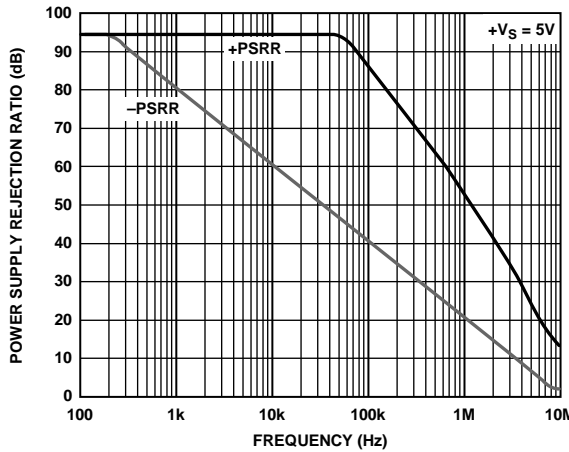


Figure 26. Power Supply Rejection Ratio vs. Frequency

09439-526

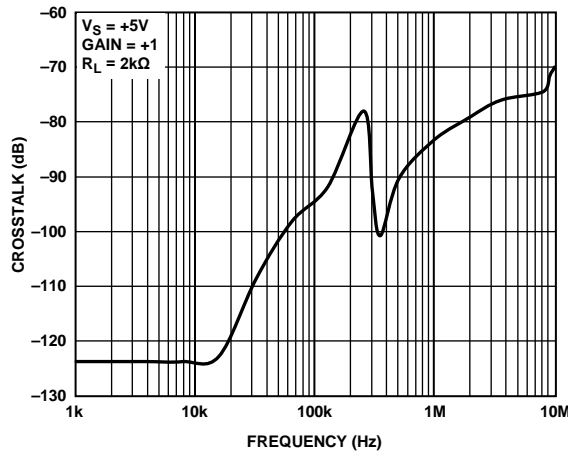


Figure 29. Crosstalk vs. Frequency

09439-063

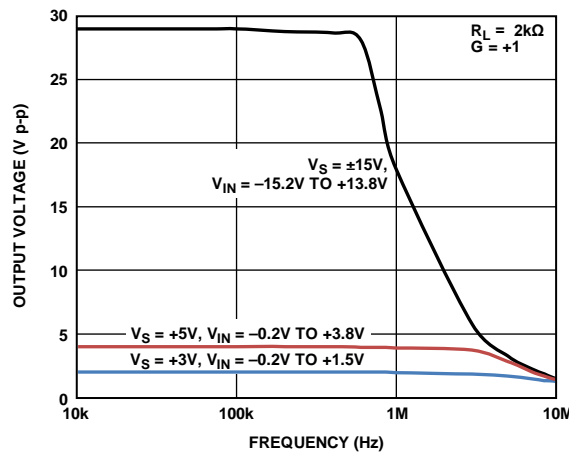


Figure 27. Large Signal Frequency Response

09439-125

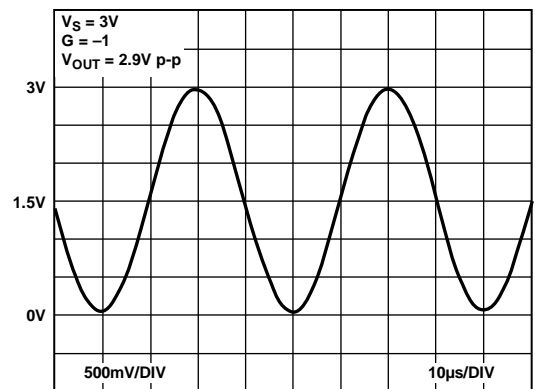


Figure 30. Output Swing, $+V_S = \pm 1.5 V$, $G = -1$

09439-025

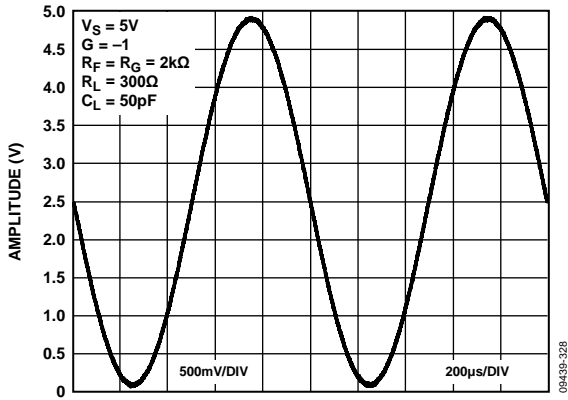


Figure 31. Output Swing, $+V_S = +5V$, $G = -1$

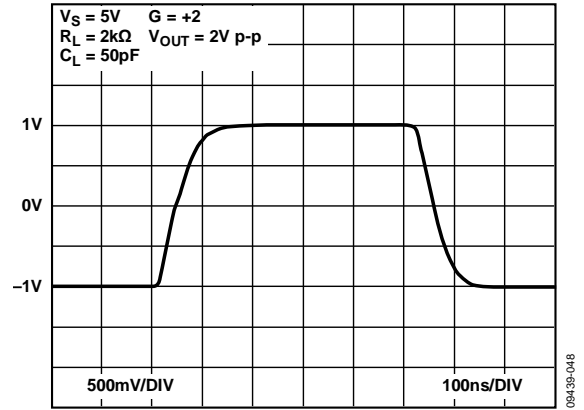


Figure 34. Pulse Response, $+V_S = \pm 2.5V$, $G = +2$

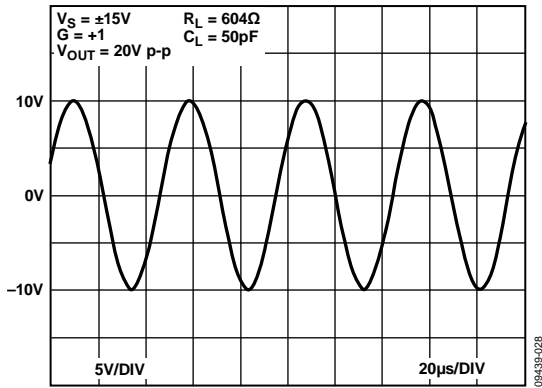


Figure 32. Output Swing, $V_S = \pm 15V$, $G = +1$

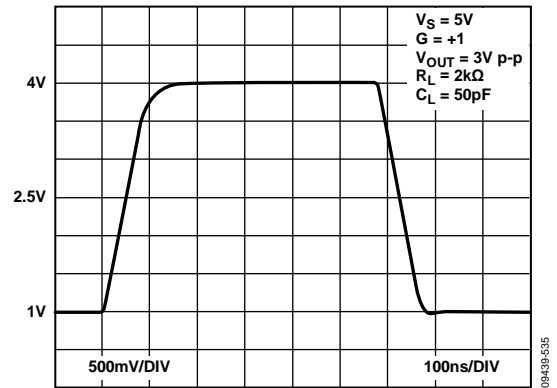


Figure 35. Pulse Response, $+V_S = \pm 2.5V$, $G = +1$

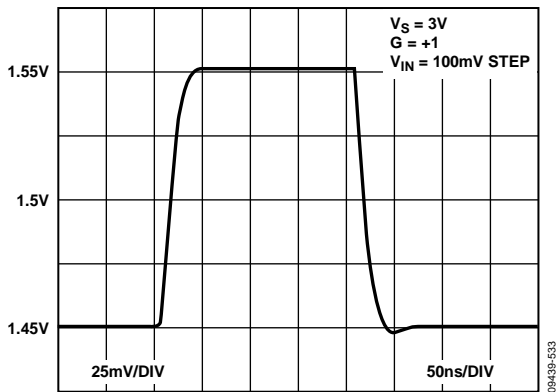


Figure 33. Pulse Response, $+V_S = \pm 3V$, $G = +1$

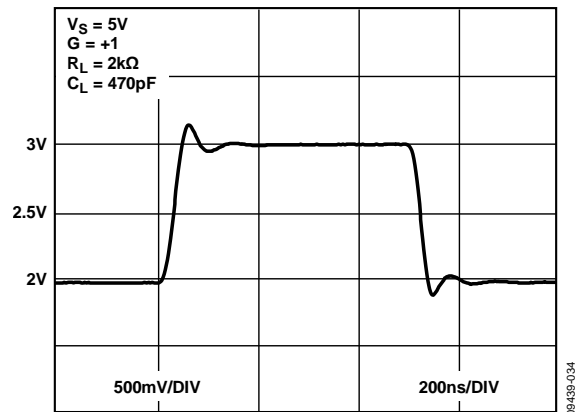


Figure 36. Pulse Response, $+V_S = +5V$, $G = +1$, $C_L = 470pF$

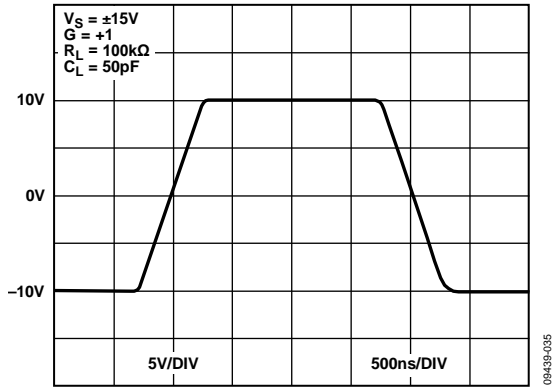


Figure 37. Pulse Response, $V_S = \pm 15V$, $G = +1$

THEORY OF OPERATION

The **AD823A** is a dual voltage feedback amplifier with an N-channel JFET input stage and a rail-to-rail bipolar output stage. It is fabricated on the Analog Devices, Inc. XFCB process, a dielectrically isolated complementary bipolar process featuring high speed 36 V bipolar devices along with JFETs and thin film resistors. The N-channel input stage handles signals up to 200 mV below the negative supply while maintaining picoamp level input currents. The rail-to-rail output maximizes the amplifier's output range and can provide up to 40 mA linear drive current with output voltages within .5 V of either power rail. Laser-trimmed thin film resistors are used to optimize offset voltage (3.5 mV max over the entire supply range) and offset voltage drift (typical 1 $\mu\text{V}/^\circ\text{C}$).

Figure 38 shows the architecture of an amplifier. Two stages are used, with the first stage folded cascode input driving the differential input of the second stage output. The voltage swing at nodes S1p and S1n are kept small to minimize the generation of nonlinear currents due to junction capacitances. This improves distortion performance. Inputs and outputs of the amplifier are fully protected with dedicated ESD diodes.

OUTPUT IMPEDANCE

The low frequency open-loop output impedance of the common-emitter output stage used in this design is approximately 50 k Ω . Although this is significantly higher than a typical emitter follower output stage, when it is connected with feedback, the open-loop gain of the op amp reduces the output impedance.

With 105 dB of open-loop gain, the output impedance is reduced to $<0.01 \Omega$. At higher frequencies, the output impedance rises as the open-loop gain of the op amp drops; however, the output also becomes capacitive due to the integrator capacitor. This prevents the output impedance from ever becoming excessively high (see Figure 21), which can cause stability problems when driving capacitive loads. In fact, the **AD823A** has excellent capacitive load drive capability for a high frequency op amp.

Figure 36 shows the results of the **AD823A** connected as a follower while driving a 470 pF direct capacitive load. Under these conditions, the phase margin is approximately 35°. For a greater phase margin, use a low value resistor in series with the output to decouple the effect of the load capacitance from the op amp (see Figure 28). In addition, running the part at higher gains also improves the capacitive load drive capability of the op amp.

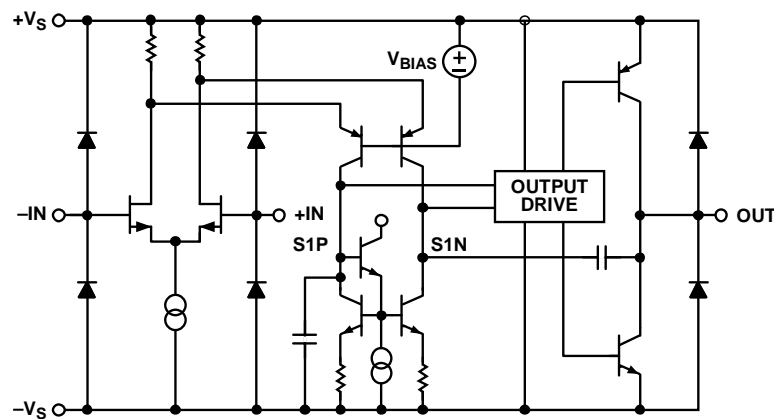


Figure 38. Simplified Schematic

09439-138

APPLICATIONS INFORMATION

INPUT CHARACTERISTICS

In the AD823A, N-channel JFETs provide a low offset, low noise, high impedance input stage. Minimum input common-mode voltage extends from 0.2 V below $-V_S$ to $1.2 V < +V_S$. Driving the input voltage closer to the positive rail causes a loss of amplifier bandwidth and increased common-mode voltage error.

The AD823A does not exhibit phase reversal for input voltages up to and including $+V_S$. Figure 39 shows the response of an AD823A voltage follower to a 0 V to 5 V ($+V_S$) square wave input. The input and output are superimposed. The output polarity tracks the input polarity up to $+V_S$, with no phase reversal. The reduced bandwidth above a 4 V input causes the rounding of the output waveform. For input voltages greater than $+V_S$, a resistor (R_P) in series with the AD823A noninverting input prevents phase reversal, at the expense of greater input voltage noise. The value of R_P ranges from 1 k Ω to 10 k Ω . This is illustrated in Figure 40.

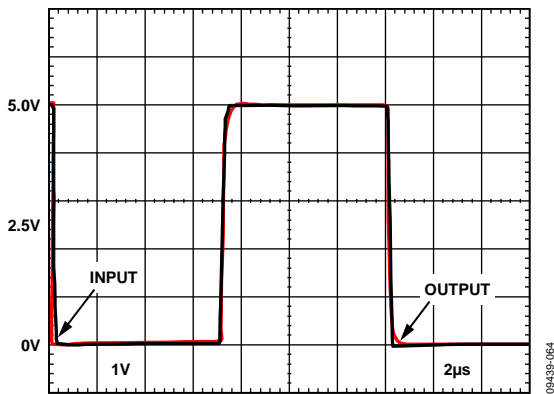


Figure 39. Input and Output Response: $R_P = 0 \text{ k}\Omega$, $V_{IN} = 0 \text{ V to } +V_S$

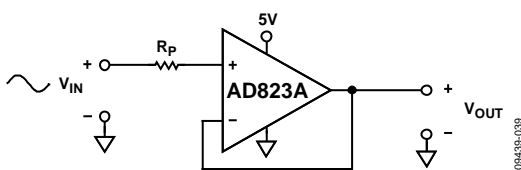
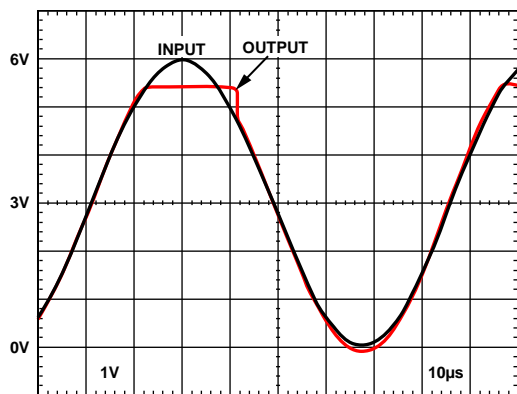


Figure 40. Input and Output Response: $V_{IN} = 0 \text{ V to } +V_S + 1 \text{ V}$, $V_{OUT} = 0 \text{ V to } +V_S + 400 \text{ mV}$, $R_P = 4.99 \text{ k}\Omega$

Because the input stage uses N-channel JFETs, input current during normal operation is negative; the current flows out from the input terminals. If the input voltage is driven more positive than $+V_S - 0.7 \text{ V}$, the input current reverses direction as internal device junctions become forward biased. This is illustrated in Figure 11.

A current limiting resistor should be used in series with the input of the AD823A if the input voltage can be driven over 300 mV more positive than $+V_S$ or 300 mV more negative than $-V_S$. The amplifier will be damaged if either condition persists for more than 10 seconds. A 1 k Ω resistor in series with the AD823A input allows the amplifier to withstand up to 10 V of continuous overvoltage and increases input voltage noise by a negligible amount.

The AD823A is designed for 14 nV/ $\sqrt{\text{Hz}}$ wideband input voltage noise (see Figure 19). This noise performance, along with the AD823A low input current and current noise, means that the AD823A contributes negligible noise for applications with high source resistances. Figure 41 shows that the source resistance contributes to negligible noise for source impedances lower than 10 k Ω . The low input capacitance of 0.6 pF also means that one can use a source impedance up to 13 k Ω without cutting into the $G = +1$ small signal bandwidth region.

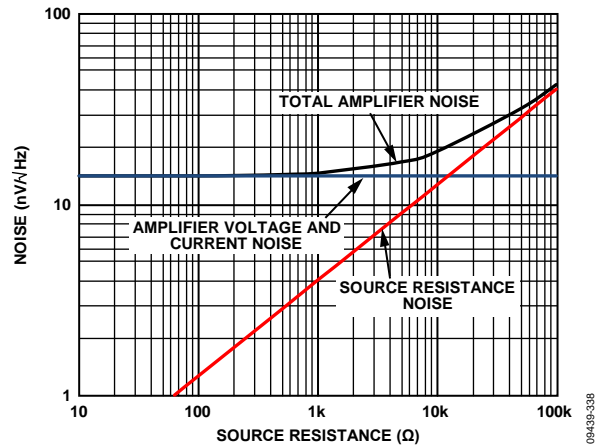


Figure 41. RTI Noise vs. Source Resistance

OUTPUT CHARACTERISTICS

The unique bipolar rail-to-rail output stage of the amplifier swings within 20 mV of the supplies with no external resistive load.

The approximate output saturation resistance of the AD823A is 33 Ω sourcing and sinking. This can be used to estimate the output saturation voltage when driving heavier current loads. For instance, when driving 5 mA, the saturation voltage to the rails is approximately 165 mV.

WIDEBAND PHOTODIODE PREAMP

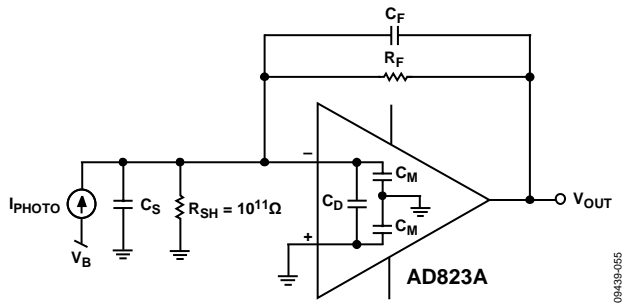


Figure 42. Wideband Photodiode Preamp

The AD823A is an excellent choice for photodiode preamp application. Its low input bias current minimizes the DC error at the preamp output. In addition, its high gain bandwidth product and low input capacitance maximizes the signal bandwidth of the photodiode preamp. Figure 42 shows the AD823A as a current-to-voltage (I/V) converter with an electrical model of a photodiode.

The transimpedance gain of the photodiode preamp can be described by the basic transfer function:

$$V_{OUT} = \frac{I_{PHOTO} \times R_F}{1 + sC_F R_F} \quad (1)$$

where I_{PHOTO} is the output current of the photodiode, and the parallel combination of R_F and C_F sets the signal bandwidth (see the I to V gain curve in Figure 43). Note that one should set R_F such that the maximum attainable output voltage corresponds to the maximum diode current I_{PHOTO} . This allows one to utilize the full output swing.

The signal bandwidth that is attainable with this preamp is a function of R_F , the gain bandwidth product (f_u) of the amplifier, and the total capacitance at the amplifier summing junction,

including C_S and the amplifier input capacitance C_D and C_M . R_F and the total capacitance produce a pole with loop frequency (f_p).

$$f_p = \frac{1}{2\pi R_F C_S} \quad (2)$$

With the additional pole from the amplifier's open loop response, the two-pole system results in peaking and instability due to an insufficient phase margin (Figure 43(A), Without Compensation).

Adding C_F creates a zero in the loop transmission that compensates for the effect of the input pole. This stabilizes the photodiode preamp design because of the increased phase margin. It also sets the signal bandwidth (Figure 43(B), With Compensation). The signal bandwidth and the zero frequency are determined by

$$f_z = \frac{1}{2\pi R_F C_F} \quad (3)$$

Setting the zero at the frequency f_x maximizes the signal bandwidth with a 45° phase margin. Since f_x is the geometric mean of f_p and f_u , it can be calculated by

$$f_x = \sqrt{f_p \times f_u} \quad (4)$$

Combining Equation 2, Equation 3 and Equation 4, the value of C_F that produces f_x is defined by

$$C_F = \sqrt{\frac{C_S}{2\pi \times R_F \times f_u}} \quad (5)$$

The frequency response in this case shows about 2 dB of peaking and 15% overshoot. Doubling C_F and cutting the bandwidth in half results in a flat frequency response with about 5% transient overshoot.

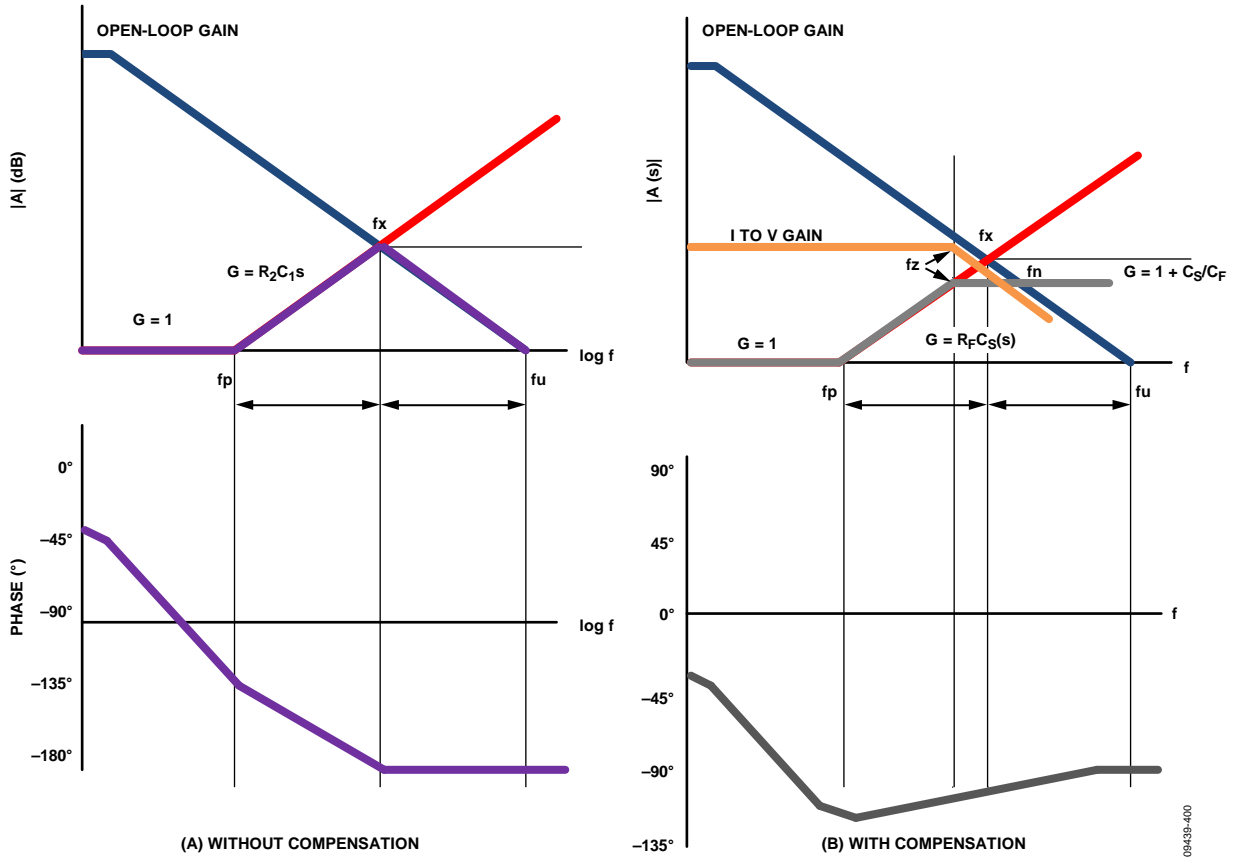


Figure 43. Gain and Phase Plot of the Transimpedance Amplifier Design

The dominant sources of output noise in the wideband photodiode preamp design are the input voltage noise of the amplifier, V_{NOISE} and the resistor noise due to R_F . The gray curve in Figure 43 shows the noise gain over frequencies for the photodiode preamp. The noise bandwidth is at the frequency f_N , and it can be calculated by

$$f_N = \frac{f_u}{(C_S + C_F)/C_F} \quad (6)$$

Figure 44 shows the AD823A configured as a transimpedance photodiode amplifier. The amplifier is used in conjunction with a photodiode detector with input capacitance of 5 pF. Figure 45 shows the transimpedance response of the AD823A when I_{PHOTO} is 1 μA p-p. The amplifier has a bandwidth of 2.2 MHz when it is maximized for a 45° phase margin with $C_F = 1.2$ pF. Note that with the PCB parasitics added to C_F , the peaking is only 0.5 dB and the bandwidth is slightly reduced. Increasing C_F to 2.7 pF completely eliminates the peaking. However, it reduces the bandwidth to 1.2 MHz.

Table 8 shows the noise sources and total output noise for the photodiode preamp, where the preamplifier is configured to have a 45° phase margin for maximal bandwidth and $f_z = f_x = f_n$ in this case.

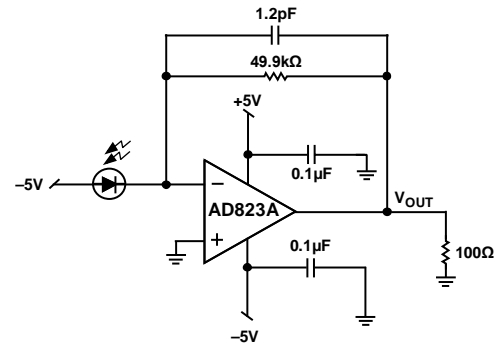


Figure 44. Photodiode Preamplifier

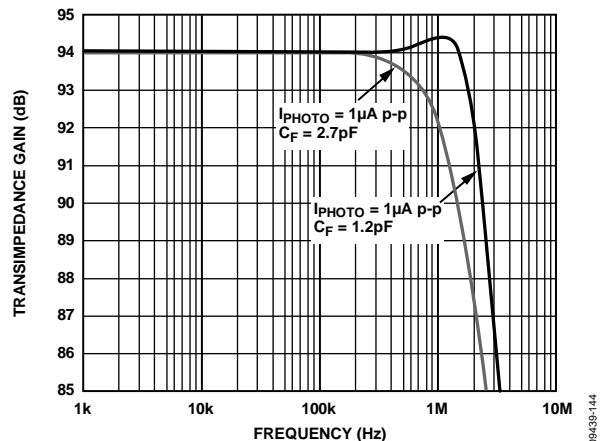


Figure 45. Photodiode Preamplifier Frequency Response

Table 8. RMS Noise Contributions of Photodiode Preamp

Contributor	Expression	(μV) ¹
R_F	$\sqrt{4kT \times R_F \times f_N \times \frac{\pi}{2}}$	55.17
V_{NOISE}	$V_{NOISE} \times \sqrt{\frac{(C_S + C_M + C_F + 2C_D)}{C_F}} \times \sqrt{\frac{\pi}{2} \times f_N}$	138.5
	RSS Total	149.1

¹RMS noise with $R_F = 50 \text{ k}\Omega$, $C_S = 5 \text{ pF}$, $C_F = 1.2 \text{ pF}$, $C_M = 1.3 \text{ pF}$, and $C_D = 0.6 \text{ pF}$.

ACTIVE FILTER

The AD823A is an ideal candidate for an active filter because of its low input bias current and its low input capacitance. Low input bias current reduces dc error in the signal path while low input capacitance improves the accuracy of the active filter.

As a general rule of thumb, the bandwidth of the amplifier should be at least 10 times bigger than the cutoff frequency of the filter implemented. Therefore, the AD823A is capable of implementing active filters of up to 1.7 MHz.

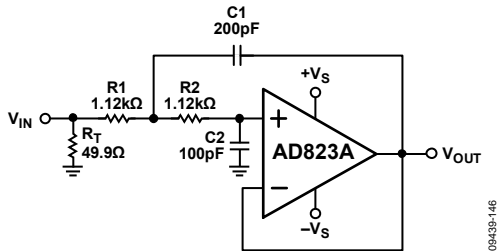


Figure 46. Two-Pole Sallen-Key Active Filter

Figure 46 shows an example of a second-order Butterworth filter, which is implemented by the Sallen-Key topology. This structure can be duplicated to produce higher-order filters.

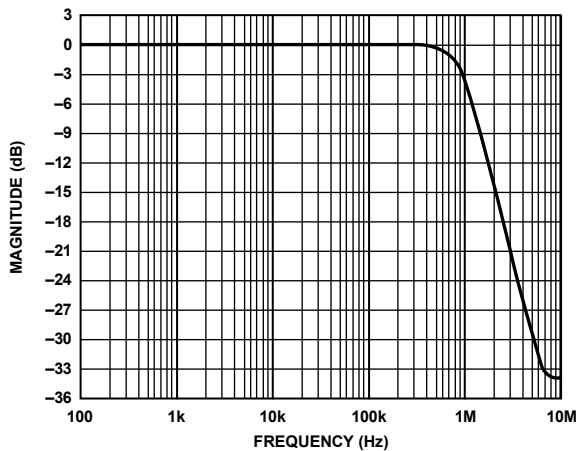


Figure 47. Two-Pole Butterworth Active Filter Response

Figure 47 shows the two-pole Butterworth active filter's response. Note that it has a maximally flat pass band, a -3 dB bandwidth of 1 MHz, and a 12 dB/octave roll-off in the stop band.

The cutoff frequency (f_c) and the Q factor of the Butterworth filter can be calculated by:

$$f_c = \frac{1}{2\pi\sqrt{R_1 R_2 C_1 C_2}} \tag{7}$$

$$Q = \frac{\sqrt{R_1 R_2 C_1 C_2}}{(R_1 + R_2) \times C_2} \tag{8}$$

Therefore, one can easily adjust the cutoff frequency by appropriately factoring the resistor and capacitor values. For example, a 100 kHz filter can be implemented by increasing the values of R1 and R2 by 10 times. Note that the Q factor remains the same in this case.

MAXIMIZING PERFORMANCE THROUGH PROPER LAYOUT

To achieve the maximum performance of the extremely high input impedance and low offset voltage of the AD823A, care should be taken in the circuit board layout. The PCB surface must remain clean and free of moisture to avoid leakage currents between adjacent traces. Surface coating of the circuit board reduces surface moisture and provides a humidity barrier, reducing parasitic resistance on the board. The use of guard rings around the amplifier inputs further reduces leakage currents. Figure 48 shows how the guard rings should be configured, and Figure 49 shows the top view of how a surface-mount layout can be arranged. The guard ring does not need to be a specific width, but it should form a continuous loop around both inputs. By setting the guard ring voltage equal to the voltage at the non-inverting input, parasitic capacitance is minimized as well. For further reduction of leakage currents, components can be mounted to the PCB using Teflon® standoff insulators.

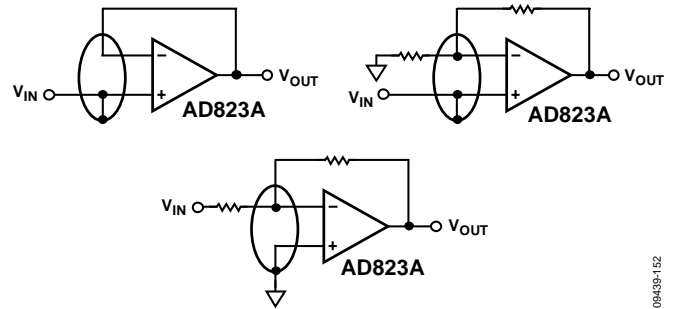


Figure 48. Guard Ring Layout and Connections to Reduce PCB Leakage Currents

09439-152

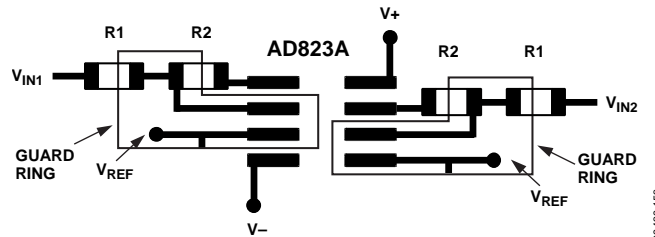
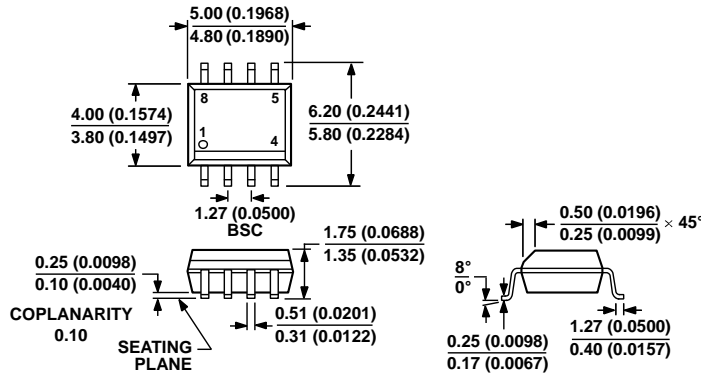


Figure 49. Top View of AD823A SOIC Layout with Guard Rings

09439-153

OUTLINE DIMENSIONS

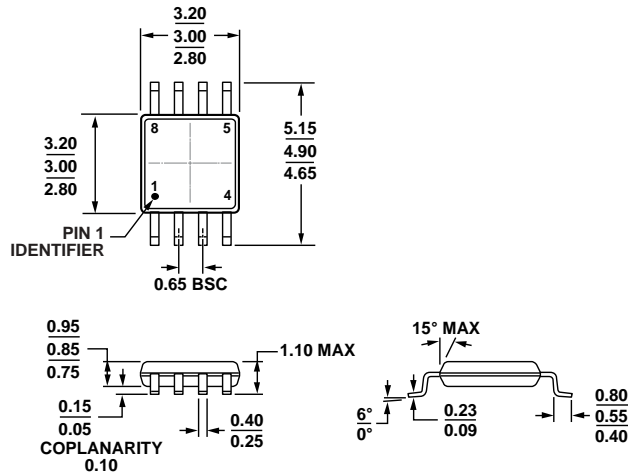


COMPLIANT TO JEDEC STANDARDS MS-012-AA
 CONTROLLING DIMENSIONS ARE IN MILLIMETERS; INCH DIMENSIONS
 (IN PARENTHESES) ARE ROUNDED-OFF MILLIMETER EQUIVALENTS FOR
 REFERENCE ONLY AND ARE NOT APPROPRIATE FOR USE IN DESIGN.

Figure 50. 8-Lead Standard Small Outline Package [SOIC_N]
 Narrow Body
 (R-8)

Dimensions shown in millimeters and (inches)

012407-A



COMPLIANT TO JEDEC STANDARDS MO-187-AA

Figure 51. 8-Lead Mini Small Outline Package [MSOP]
 (RM-8)

Dimensions shown in millimeters

10-07-2009-B

ORDERING GUIDE

Models ¹	Temperature Range	Package Description	Package Option	Branding
AD823AARZ	-40°C to +85°C	8-Lead SOIC_N	R-8	
AD823AARZ-RL	-40°C to +85°C	8-Lead SOIC_N, 13" Tape and Reel	R-8	
AD823AARZ-R7	-40°C to +85°C	8-Lead SOIC_N, 7" Tape and Reel	R-8	
AD823AARMZ	-40°C to +85°C	8-lead MSOP	RM-8	H34
AD823AARMZ-R7	-40°C to +85°C	8-lead MSOP, 7" Tape and Reel	RM-8	H34
AD823A-2AR-EBZ		Evaluation Board for 8-Lead SOIC		
AD823A-2ARM-EBZ		Evaluation Board for 8-Lead MSOP		

¹ Z = RoHS Compliant Part.